Nuclear Physics A457 (1986) 351-366
North-Holland, Amsterdam

MICROSCOPIC POTENTIAL MODEL STUDIES OF LIGHT NUCLEAR CAPTURE REACTIONS

K. LANGANKE

Institut für Theoretische Physik I, Universität Münster, West Germany

Received 12 March 1986

Abstract: We have studied the astrophysically important $^{2}H(\alpha, \gamma)^{6}Li$, $^{3}H(\alpha, \gamma)^{7}Li$, and $^{3}He(\alpha, \gamma)^{7}Be$ reaction in the framework of a microscopic potential model. Our capture cross sections reproduce the experimental data at low energies in all three cases. While for the $^{2}H(\alpha, \gamma)^{6}Li$ and $^{3}He(\alpha, \gamma)^{7}Be$ reactions our results support the astrophysical conclusions based on the currently accepted reaction rates, we predict for the $^{3}H(\alpha, \gamma)^{7}Li$ reaction a thermally averaged reaction rate which is higher at temperatures $T = (1\text{-}10) \times 10^{8}$ K than presently recommended.

1. Introduction

In stars charged-particle nuclear reactions proceed at such low energies that a direct experimental determination of the cross section required for studies of stellar nucleosynthesis is not possible in the laboratory with existing techniques. Hence an extrapolation down to stellar energies of cross sections measured at energies accessible in the laboratory is usual and necessary in nuclear reactions of astrophysical interest. In order not to be unreliable such an extrapolation should have a strong theoretical foundation and should be based on as much experimental information as possible. If the nuclear reactions to be studied at stellar energies involve bound states or resonant states of the combined system many-particle effects caused by the Pauli principle and the internal structure of the fragment nuclei might become quite important and should be considered in the extrapolation procedure.

The description of nuclear reactions important in astrophysics requires very often the study of two-fragment systems of light nuclei at low energies. It is well known [1,2]) that many-body reaction theories like the resonating group method (RGM) or the generator coordinate method (GCM) are good tools for the study of nuclear reactions with a small number of nucleons and at low energies, where few reaction channels are involved. Hence the study of astrophysically important light nuclear reactions seems to be the ideal field for applications of the RGM and GCM. However, one has to keep in mind that any useful description of nuclear reactions important for nucleosynthesis in stars requires a careful and accurate account of physically relevant input data, especially of energy positions and widths of resonances and bound states which happen to fall into the stellar energy range or to dominate the reaction rate

in this very regime. Consequently a physically accurate description of the nuclear reactions becomes more important than a microscopically pure derivation of cross sections from first principles. Hence the most reasonable compromise seems to be the consistent incorporation of the qualitative results of the microscopic theory of nuclear reactions, as e.g. they are reviewed in ref. [3]), into a reliable description which quantitatively reproduces those experimental data which are particularly important at stellar energies.

Recently a microscopic potential model has been suggested for the study of light nuclear reactions at stellar energies [4,5]). This model, which is based on the qualitative results of the many-body RGM or GCM, combines the basic ingredients of a microscopic many-body theory by the use of antisymmetrized many-body wave functions with the flexibility of a phenomenological potential model with adjustable potential parameters. The parameters may be used to reproduce physically relevant input data to make the study meaningful for the subsequent use in models of stellar nucleosynthesis.

The microscopic potential model was first applied [4,5]) to the astrophysically very important electromagnetic capture reaction of α-particles on ^{12}C [see refs. [6-8])] whose reaction rate at stellar energies is experimentally rather uncertain [9-11]).

In order to place more confidence into the theoretical studies of the $^{12}C(\alpha, \gamma)^{16}O$ reaction we want to demonstrate in this paper that the microscopic potential model is able to describe the astrophysically also important electromagnetic capture of α-particles on ^{2}H, ^{3}H and ^{3}He. As physically relevant input data we have adjusted the nucleus-nucleus potentials in the various studies to reproduce the energy positions of bound states and resonances at stellar energies as well as the experimentally known phase shifts at low energies.

The paper is organized as follows. In sect. 2 we give a description of the microscopic potential model for electromagnetic capture reactions. In sect. 3 we report about its application to the $^2H(\alpha, \gamma)^6Li$ reaction, the $^3H(\alpha, \gamma)^7Li$ reaction and the $^3He(\alpha, \gamma)^7Be$ reaction, at stellar energies. Additionally to the description of the various microscopic potential model studies, we also discuss possible consequences of the calculated stellar reaction rates in astrophysical applications, which might be most intriguing in the case of the $^3H(\alpha, \gamma)^7Li$ reaction.

2. The microscopic potential model

A detailed description of the microscopic potential model as well as its justification on the basis of the microscopic many-body scattering theories like RGM and GCM is given in ref. [3]). In this chapter we want to give a synopsis of the model for the one-channel case as this seems to be sufficient for a meaningful study of the electromagnetic capture reactions discussed in this paper. An extension of the model to the coupled-channel case including excitations of the fragment nuclei was presented in ref. [12]).

With the restriction to a single two-fragment channel the model space in the present studies is spanned by antisymmetrized many-body wave functions of the form*

$$\Psi_{JII}(\boldsymbol{x}) = \mathscr{A}\{\{[\Phi_\alpha \Phi_{2,I}]_I Y_l(\hat{\boldsymbol{x}})\}_J g_{JI}(x)\} . \tag{2.1}$$

The Φ_α, $\Phi_{2,I}$ are harmonic oscillator wave functions describing the internal degrees of freedom of the α-particle and the second fragment which in the present calculation is either a deuteron, a triton or a ^{3}He nucleus. The channel spin I, which in (2.1) is given by the deuteron ($I=1$) or by the triton or the ^{3}He nucleus ($I=\frac{1}{2}$), and the relative orbital angular momentum l are coupled to the total angular momentum J. Note that microscopic RGM studies revealed the two-cluster wave functions as defined in (2.1) to be the dominant configurations of the low-energy spectra in all the three relevant combined systems: ^{6}Li, ^{7}Li and ^{7}Be [refs. [13-15])]. Deviating from these more elaborate calculations [13-15]) we assume that the two-cluster wave functions in (2.1) have identical oscillator parameters. For simplicity we have adopted the value $b = 1.525$ fm from the $^3\mathrm{H}+\alpha$ study of ref. [16]) for all calculations.

Having fixed the internal structure of the fragments the unknown wave functions of relative motion $g_{JI}(x)$ can be determined by solving the Schrödinger-like equation of relative motion

$$\Lambda_l \left\{ -\frac{\hbar^2}{2\mu x} \frac{\mathrm{d}^2}{\mathrm{d}x^2} x + V_{JI}(x) + V_c(x) + \frac{l(l+1)\hbar^2}{2\mu x^2} - E \right\} \Lambda_l \tilde{g}_{JI}(x) = 0 \tag{2.2}$$

and via the transformation

$$g_{JI}(x) = \sum_N \mu_N^{-1/2} \langle u_N^l \,|\, \tilde{g}_{JI} \rangle u_N^l(x) . \tag{2.3}$$

The normalization constants μ_N are different for the various nuclear systems considered in the present studies but for the class of wave functions defined in (2.1) they do not depend on angular momenta and are known analytically [17]). The u_N^l are spherical oscillator wave functions with main quantum number $N = 2n + l$ and width $\beta = b/\sqrt{\mu}$, where μ is the reduced mass parameter. Substituting the expansion (2.3) into (2.1) ensures the orthogonality of the many-body states (2.1). The Pauli projectors Λ_l in (2.2) guarantee that Ψ_{JII} will not have components which violate the Pauli principle [18-19]). Note that this requirement of orthogonality on the Pauli-forbidden states introduces a nodal structure in the relative wave functions which is an important feature of microscopic studies of composite particle reactions [18-20]). Moreover, Baye and Descouvemont have demonstrated recently that an appropriate nodal structure of the relative wave functions has to be an indispensable ingredient of any meaningful study of electromagnetic capture reactions at low energies [21]). However, it is often not considered in phenomenological potential model studies.

* To simplify notation we have suppressed the index m for the magnetic quantum number throughout this paper.

As has been discussed above, the potentials in (2.2) will be determined to reproduce the energy positions (and widths) of the low-lying states in the spectrum of the combined systems as well as the experimentally known phase shifts at low energies. For light nuclear systems the nuclear potentials [19,22]) as well as the spin-orbit potential [23]) have been found to be well approximated by a local, l-dependent form which for convenience was chosen as a sum of a few Gaussians. In the present paper, however, we adopted a Saxon-Woods form factor motivated by the $\alpha+d$ potential of ref. [24]). Hence,

$$V_{Jl}(x)=(W_l+W_s\boldsymbol{l}\cdot\boldsymbol{s})f(x)\,,\qquad f(x)=\{1+\exp\{(x-R)/a\}\}^{-1}\,. \tag{2.4}$$

The Coulomb potential might be approximated by that of homogeneously charged sphere [19]) where the radius $R_c=1.83$ fm has been adopted from the phenomenological $\alpha+$d potential of ref. [24]).

The many-body states (2.1) are derived by calculating its relative part from the solution of eq. (2.2) subject to appropriate boundary conditions. For scattering states these boundary conditions were chosen as

$$g_{Jl}(x)\to\frac{1}{kx}\sqrt{\frac{(2l+1)4\pi}{v}}(\cos\delta_l F_l(kr)+\sin\delta_l G_l(kr)) \tag{2.5}$$

to guarantee unit flux in the entrance channel. In (2.5), k and v are the wave number and the relative velocity, δ_l are the nuclear phase shifts and F_l, G_l denote the regular and irregular Coulomb functions.

The capture cross section from a scattering state $\Psi_{Jll}(E)$ into a bound state $\Psi_{J'l'I'}$ via an electromagnetic transition operator of multipolarity λ (for the present studies it is sufficient to consider only the electric case) is given in the long-wavelength approximation and in first-order perturbation theory by [25])

$$\sigma_{JJ'}^{ll'II'}(E)=\frac{8\pi(\lambda+1)}{\hbar\lambda((2\lambda+1)!!)^2}\left(\frac{E_\gamma}{\hbar c}\right)^{2\lambda+1}\frac{1}{2J+1}|\langle\Psi_{Jll}(E)\|Q_\lambda\|\Psi_{J'l'I'}\rangle|^2\,. \tag{2.6}$$

Here E_γ is the energy of the emitted photon and Q_λ is the electric many-body transition operator. The total capture cross section $\sigma(E)$ is given by summing over all relevant partial cross sections $\sigma_{JJ'}^{ll'II'}(E)$.

For the capture reactions studied in this paper it is sufficient to consider only electric dipole transitions (^{3}H(α, γ)^{7}Li, ^{3}He(α, γ)^{7}Be) and the isoscalar part of the electric quadrupole transition (^{2}H(α, γ)^{6}Li). Hence the many-body matrix elements required in the evaluation of (2.6) are most conveniently calculated using a technique proposed by Suzuki [26]) which is based on a decomposition of the relevant transition operators into parts acting only on the internal coordinates of the two fragment nuclei and a part which acts on the relative coordinate between the fragments. Due to various selection rules [see e.g. refs. [4,26,27])] the internal parts of the operators do not contribute to the many-body matrix elements in the present cases. Explicit

cross-section formulae relevant for the calculation of the stellar capture rate will be given in sect. 3 when discussing the individual capture reactions.

3. Results

In this section we want to present the results of the microscopic potential model studies of the ^{2}H(α, γ)^{6}Li, ^{3}H(α, γ)^{7}Li, and ^{3}He(α, γ)^{7}Be reactions at stellar energies. The calculations are restricted to the dominant type of radiation only. This section mainly emphasizes the description of the potential model studies. However, a brief discussion of the astrophysical background of the various reactions as well as of possible consequences of the present calculations will be given.

3.1. THE ^{2}H(α, γ)^{6}Li REACTION AT STELLAR ENERGIES

The ^{2}H(α, γ)^{6}Li reaction is the only mechanism likely to produce ^{6}Li within the big bang. However, first estimates of the reaction rate in the relevant stellar energy range ($E < 1$ MeV) revealed that the rate is very small [28]), mainly caused by the fact that E1 and M1 multipole radiation is strongly hindered at stellar energies and the reaction rate is dominated by E2 radiation. Based on an estimation of the direct capture cross section and the resonant transition from the $J = 3^+$ resonance at $E = 0.711$ MeV into the only ^{6}Li bound state at $E = -1.4753$ MeV [ref. [29])], it was concluded that the ^{2}H(α, γ)^{6}Li rate is too low to produce a significant amount of the ^{6}Li abundancy during the big bang. Hence, it is generally believed that ^{6}Li is made via the galactic cosmic rays [30]).

The theoretical estimate has subsequently been supported by an experimental measurement of the ^{2}H(α, γ)^{6}Li cross section in the energy range $E = 1$–4 MeV [ref. [30])]. The experimental data could be understood in terms of a direct capture model in which the electromagnetic transition occurs as E2 radiation from $\alpha + d$ scattering states (including the $J = 3^+$ resonance) into the ^{6}Li ground state which was described as a bound state in the $\alpha + d$ s-wave. In the study of ref. [30]) the scattering states as well as the bound state were derived from the phenomenological McIntyre–Haeberli potential [24]) which was fitted to reproduce the elastic $\alpha + d$ phase shifts. The potential depth in the s-wave was adjusted to yield the correct binding energy of the ^{6}Li ground state.

However, in order to fit the experimental data the theoretical capture rate had to be normalized by an overall factor of 0.85 which was interpreted as the spectroscopic overlap between the ^{6}Li ground state and an $\alpha + d$ cluster configuration [30]). In the following we want to demonstrate that the experimental ^{2}H(α, γ)^{6}Li capture cross section can be reproduced in an excellent quality on the basis of the microscopic potential model, if, in contrast to ref. [30]), microscopic many-body cluster functions are used and the influence of the Pauli principle on the relative wave functions of the clusters is considered.

As mentioned above the $^2H(\alpha, \gamma)^6Li$ reaction rate at stellar energies is given by the radiative E2 capture from the d-scattering waves in the $\alpha + d$ channel, including the $J = 3^+$ resonance at $E = 0.711$ MeV, into the ^6Li ground state. The microscopic potential model study is based on the fact that all the states relevant for a study of this reaction are well described by antisymmetrized $\alpha + d$ cluster configurations [13]), whose internal wave functions were approximated by the respective harmonic oscillator ground states of the two nuclei. The relative wave functions between the clusters were calculated from eq. (2.2). Note that in the microscopic potential model the Pauli principle requires the orthogonality of the $\alpha + d$ s-wave on the harmonic oscillator shell model function $u^{l=0}_{N=0}$. The related nodal structure in the $\alpha + d$ s-waves was not considered in the phenomenological study [30]). The potential in (2.2) was described by the Coulomb potential of a homogeneously charged sphere and a nuclear part for which an ansatz closely related to the McIntyre-Haeberli potential was used. A coupling of different partial waves was neglected as this might be justified below $E \approx 5$ MeV [refs. [24,31])]. The parameter $a = 0.7$ fm was adopted from ref. [24]). The other parameters (W, W_s, R) were adjusted to reproduce the experimental phase shifts in the partial waves $(Jl) = (32)$, (22) and (12) for energies $E_d \leq 10$ MeV [ref. [31])]. These requirements were fulfilled using the parameters $W_{l=2} = -79.81$ MeV, $W_s = -3.9$ MeV and $R = 1.83$ fm. The $\alpha + d$ s-wave states including the ^6Li ground state were derived from a Gaussian potential with a depth $V_0 = -83.21$ MeV and a width $a = 2.1$ fm which was adjusted to the binding energy of the ^6Li ground state and the s-wave phase shifts. The fit to the experimental phase shifts as obtained by solving (2.2) is shown in fig. 1. Note that the binding energy of the ^6Li ground state as well as the energy of the $J = 3^+$ resonance are reproduced better than within 5 keV. The width of the 3^+ resonance is calculated as $\Gamma \approx 21$ keV, which has to be compared with the experimental value of $\Gamma \approx 24 \pm 2$ keV [ref. [32])].

The $^2H(\alpha, \gamma)^6Li$ reaction rate has been calculated on the basis of the many-body wave functions (2.1) adopting the bound state of the s-wave potential as relative wave function of the ^6Li ground state and calculating the relative wave functions of the scattering states using the potentials $W_{l=2}$.

The E2 capture cross section from an $a + d$ scattering state with quantum numbers $(J2)$ into the ^6Li ground state, is given by

$$\sigma(E) = \sum_J \sigma_J(E), \qquad \sigma_J(E) = \frac{16\pi e^2}{675\hbar v} \frac{2J+1}{3} \left(\frac{E_\gamma}{\hbar c}\right)^5 |I_2|^2, \tag{3.1}$$

where the radial matrix element is defined as

$$I_2 = \int \tilde{g}_{J2}(x) x^2 \tilde{g}_{10}(x)\, dx + \sum_{N,N'} (a_{NN'} - 1) \langle \tilde{g}_{J2} | u^2_N \rangle \langle u^0_{N'} | \tilde{g}_{10} \rangle \int u^2_N(x) x^2 u^0_{N'}(x)\, dx \tag{3.2}$$

with

$$a_{NN'} = \begin{cases} (\mu_N/\mu_{N'})^{1/2} & \text{for } N \leq N' \\ (\mu_{N'}/\mu_N)^{1/2} & \text{for } N \geq N'. \end{cases} \tag{3.3}$$

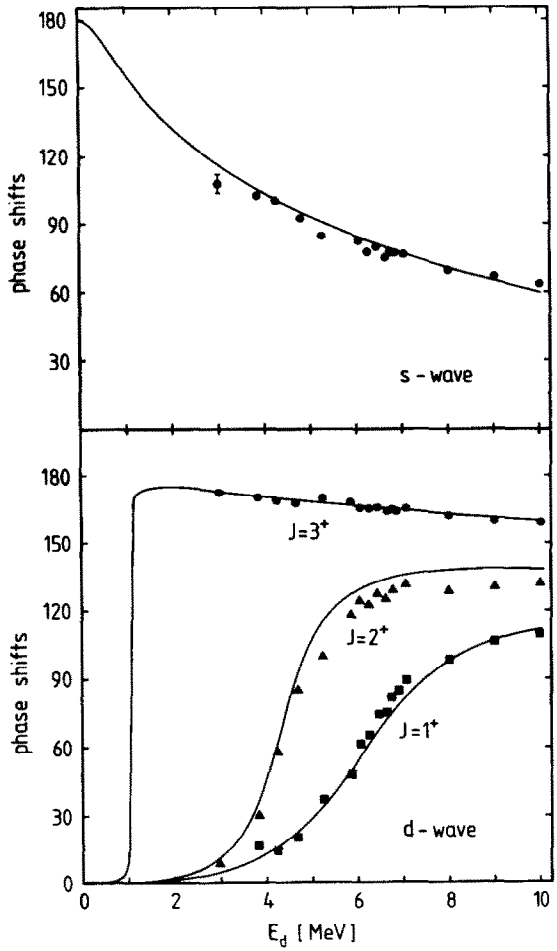

Fig. 1. Microscopic potential model fit to the experimental phase shifts [31]) in elastic $\alpha + d$ s- and d-wave scattering. The potential parameters are given in the text.

The appearance of the second term in (3.2) is a consequence of the many-body character of our calculation. The sum has to be taken over all Pauli-allowed states $(N, N' \geq 2)$ fulfilling the conditions $N' = N \pm 2$, N. Actually the sum is restricted to only a few values of N, N', since the normalization kernels, and hence $a_{NN'}$, rapidly converges against unity [17]).

The total $^2H(\alpha, \gamma)^6Li$ capture cross section for $E \leq 5$ MeV is shown in fig. 2. The agreement to the experimental data below $E \leq 3.5$ MeV is excellent. The measured cross section at $E \approx 4$ MeV, however, is not reproduced within the present microscopic potential model study. The excess of the experimental data, which was also observed in the phenomenological direct capture model fit of ref. [30]), can be attributed to capture into the $(J = 0^+, T = 1)$ state at $E = 2.09$ MeV in ^6Li which

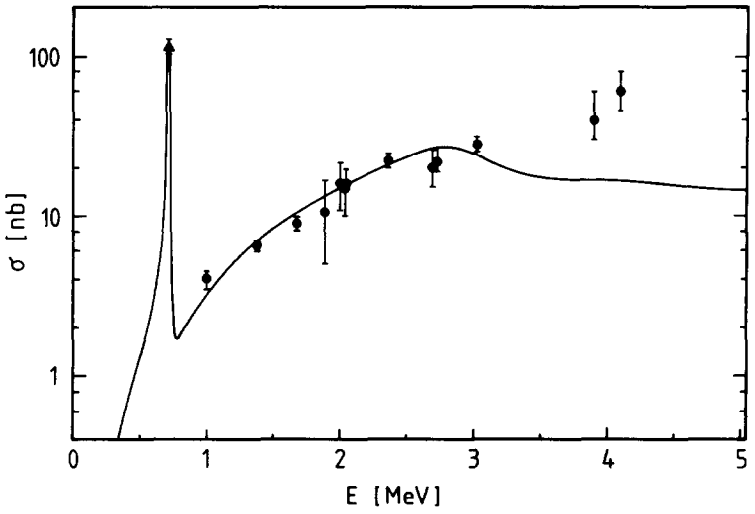

Fig. 2. Comparison of the $^2H(\alpha, \gamma)^6Li$ reaction cross section calculated in the microscopic potential model with the experimental data of Robertson *et al.* [30]).

cannot be described within the model space spanned by the $\alpha + d$ many-body cluster wave functions. The data point at the peak of the $J = 3^+$ resonance is the radiative width of this state converted into cross section. Vice versa, a parametrization of the calculated cross section in the vicinity of the $J = 3^+$ resonance by a Breit-Wigner form yields a γ-width of $\Gamma_\gamma = 4.2 \times 10^{-4}$ eV, in agreement with the experimental value [$\Gamma_\gamma = (4.4 \pm 0.34) \times 10^{-4}$ eV, ref. [32])].

On the basis of the total E2 capture cross section we have calculated the thermally averaged reaction rate [33])

$$N_A\langle\sigma v\rangle = 4.102 \times 10^{10} \mu^{-1/2} T_9^{-3/2} \times \int \sigma(E) E \exp\{-11.605 E/T_9\}\, dE [\mathrm{cm^3\, s^{-1}\, mole^{-1}}]. \quad (3.4)$$

In (3.4) the cross section σ is measured in barn, the energies are given in MeV and T_9 is the temperature in units of 10^9 K; N_A is Avogadro's number. In fig. 3 we compare our reaction rate with that given in parametrized form in ref. [30]). This rate [30]) also accounts for possible contributions of the strongly suppressed E1 radiation which, however, at the temperatures shown in fig. 3 are still dominated by the E2 contributions. It seems therefore justified to conclude from fig. 3 that a total thermally averaged reaction rate which is calculated on the basis of the present E2 capture cross section and in which for other types of radiation is properly accounted for will be lower than the rate given in ref. [30]). We believe that this is true for the whole temperature range shown in Fig. 3, particularly at $T_9 = 0.8$ which is the temperature appropriate for the ^6Li production during the big bang. Giving lower reaction rates our calculation certainly supports the important finding of

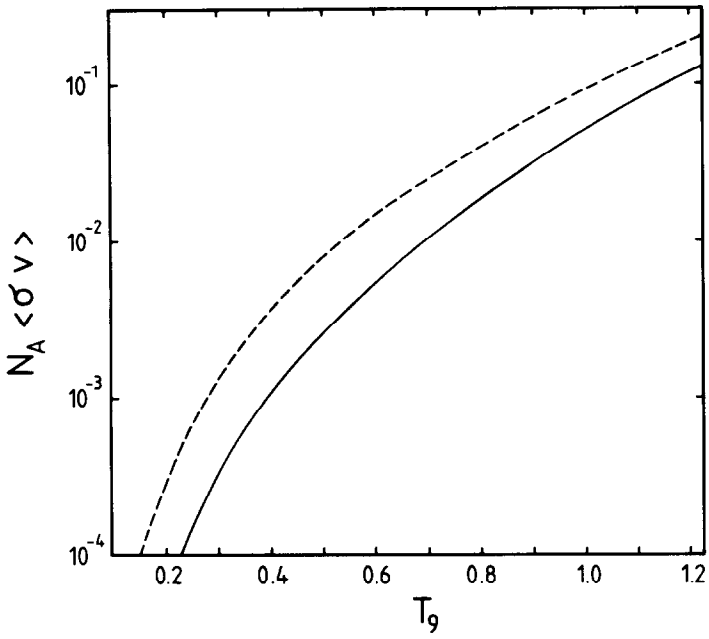

Fig. 3. Comparison of the thermally averaged ^{2}H(α, γ)^{6}Li reaction rate calculated from the present E2 capture calculation solid line with the (total) rate given in ref. [30]) (dashed).

ref. [30]) that only a very small amount of ^{6}Li (less than 2%) [30]) has been produced in the big bang.

Concluding the study of the ^{2}H(α, γ)^{6}Li reaction it should be emphasized that the calculation of the capture cross section in the microscopic potential model is parameter-free as no parameter has been adjusted to radiative capture data. An overall normalization as in the phenomenological direct capture study [30]) is not necessary, if the calculation is performed on microscopic grounds considering totally antisymmetrized cluster wave functions with internal structure. However, the consideration of the internal structure of the fragments (the second term in eq. (3.2)) is found to be less important for the $\alpha + d$ system, since all the kernels μ_N are relatively close to unity. On the other hand, the nodal structure of the relative wave function of the ^{6}Li ground state, which is required by the Pauli principle due to the orthogonality on the Pauli forbidden state $u^{l=0}_{N=0}$, reflects a basic and indispensable consequence of the microscopic many-body calculation.

3.2. THE ^{3}He(α, γ)^{7}Be CAPTURE REACTION AT STELLAR ENERGIES

The "solar-neutrino problem" has become one of the outstanding puzzles in astrophysics. Its origin is the striking difference between the theoretical predictions

about the neutrino production during the solar hydrogen burning and the much smaller neutrino flux observed in experiments. For a recent review about the solar neutrino problem see Davis and Bahcall [34]). The theoretical predictions, of course, have to rely on solar models, which require as input empirical data from different fields of physics. As it is generally accepted that the sun generates its energy by fusing hydrogen to helium, the nuclear physics input into the solar models are cross sections of nuclear reactions within hydrogen burning in the p-p chain. From the nuclear reactions involved in the solar hydrogen burning stage the ^{3}He$(\alpha, \gamma)^7$Be reaction has been discussed as a possible source of the solar neutrino problem. This process has been studied within the framework of the microscopic potential model.

The ^{3}He$(\alpha, \gamma)^7$Be reaction rate at stellar energies is in an excellent approximation given by the E1 capture from the ^{3}He$+\alpha$ s-wave and d-wave scattering states into the two ^{7}Be bound states at $E=-1.586$ MeV $(J=\frac{3}{2}^-)$ and at $E=-1.157$ MeV $(J=\frac{1}{2}^-)$ [ref. [35])]. The potential model study is based on the fact that all these states can be well described by a ^{3}He + α cluster wave function, where inelastic excitations of the fragments may be safely neglected [14,15]). The internal wave functions are adopted as the harmonic oscillator shell model ground states of ^{3}He and ^{4}He.

The relative wave functions $\tilde{g}$ were derived from (2.2), where the Pauli operator projects out the spherical oscillator wave functions u_N with $N<3$. The nuclear potential in the p-waves was approximated by the form factor (2.4). The potential parameters were adjusted to reproduce simultaneously the binding energies of the two bound states in ^{7}Be and the experimentally known $P_{3/2}$ and $P_{1/2}$ phase shifts for energies $E_\alpha \leq 16$ MeV [ref. [36])]. These requirements can be fulfilled by choosing $W_{l=1}=-81.582$ MeV, $W_s=-2.36$ MeV, $a=0.7$ fm. However, in contrast to the ^{2}H$(\alpha, \gamma)^6$Li case, different radii have been adopted for the central part ($R=2.25$ fm) and the spin-orbit part ($R=1.83$ fm) of the potential. To calculate the $l=0$ and $l=2$ scattering states in the entrance channel the microscopically derived nucleus-nucleus potential of Friedrich [16]) was adopted. Slightly changing the long-ranged part of this 2-gaussian potential to -41 MeV, one obtains an excellent reproduction of the experimental phase shifts in the positive parity partial waves for $E_\alpha \leq 15$ MeV. The fit to the experimental phase shifts in the $P_{3/2}$, $P_{1/2}$ and $S_{1/2}$ partial waves is shown in fig. 4.

The ^{3}He$(\alpha, \gamma)^7$Be E1 capture cross section at low energies is given by

$$\sigma(E)=\sum_{JJ'}\sigma_{JJ'}^{ll'}(E) \tag{3.5}$$

with

$$\sigma_{JJ'}^{ll'}(E)=\frac{32\pi e^2}{147\hbar v}\left(\frac{E_\gamma}{\hbar c}\right)^3(2J+1)(2J'+1)$$
$$\times\langle l, l'\rangle\begin{Bmatrix}1 & l & l'\\ \frac{1}{2} & J' & J\end{Bmatrix}^2|I_1|^2 . \tag{3.6}$$

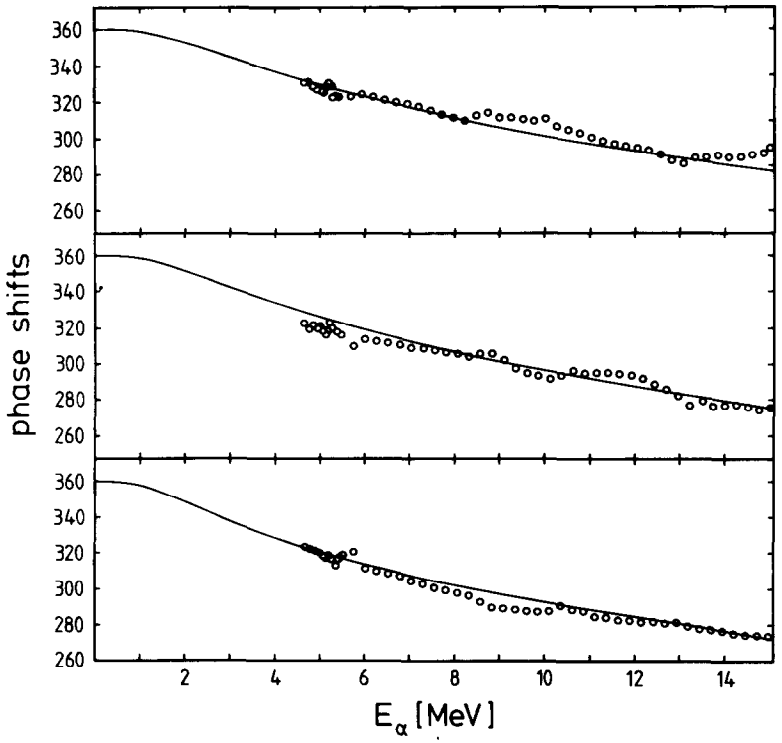

Fig. 4. Microscopic potential model fit to the experimental phase shifts [36]) in elastic ^{3}He+α $p_{3/2}$-wave (top panel), $p_{1/2}$-wave (middle panel) and $s_{1/2}$-wave (bottom panel) scattering.

In (3.6) $\langle l, l'\rangle$ means the larger of l, l' and $\{\ \}$ is the 6-j symbol. The radial integral is given by

$$I_1 = \int \tilde{g}_{Jl}(x) x \tilde{g}_{J'l'}(x)\, \mathrm{d}x + \sum_{N,N'} \langle \tilde{g}_{Jl} | u^l_N \rangle \langle u^{l'}_{N'} | \tilde{g}_{J'l'} \rangle (a_{NN'} - 1) \times \int u^l_N(x) x u^{l'}_{N'}\, \mathrm{d}x . \tag{3.7}$$

The sum in (3.7) runs over all $N, N' \geq 3$ with $N' = N \pm 1$. Again the sum is restricted to only a few terms, since the $a_{NN'}$ which are defined as in (3.3) converge rapidly to unity.

The E1 capture cross sections at energies $E = 0.1$–1.7 MeV were calculated from (3.5)-(3.7) with the relative wave functions as derived above. The cross sections are shown in fig. 5. The agreement with the experimental data in this energy range [37-39])

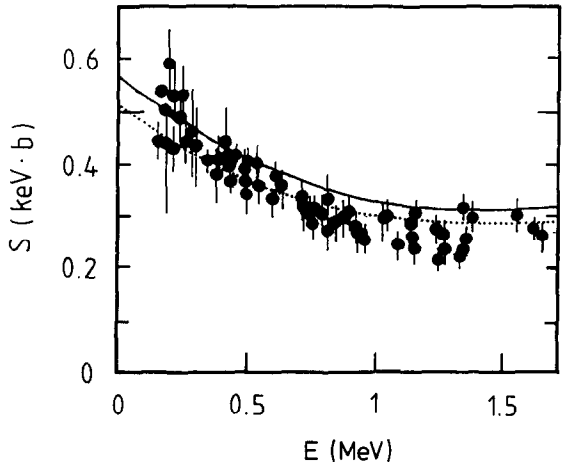

Fig. 5. Comparison of the ^{3}He(α, γ)^{7}Be astrophysical S-factor at stellar energies calculated in the microscopic potential model (solid line) and in the RGM calculation (dotted line, ref. [43])) with the experimental data [refs. [37-39])].

is fair. By extrapolating the calculated astrophysical S-factor

$$S(E) = E\sigma(E) \exp\{2\pi\eta\}, \tag{3.8}$$

where η is the Sommerfeld parameter, down into the range of astrophysical interest ($E \approx 1$–20 keV) we find $S(0) = 0.56$ keV · b. This microscopic potential model result is in fair agreement with the values empirically derived from the observation of prompt γ-rays (direct measurement) in the ^{3}He(α, γ)^{7}Be reaction ($S(0) = 0.47 \pm 0.05$ keV · b [ref. [37])], 0.58 ± 0.07 keV · b [ref. [38])], 0.52 ± 0.03 keV · b [ref. [39])], 0.47 ± 0.04 keV · b [ref. [40])] or the observation of the 478 keV γ-rays due to the transition from the $J = \frac{1}{2}^-$ level to the ground state in ^{7}Li following a positron decay of the ^{7}Be ground state (activation measurement) ($S(0) = 0.55 \pm 0.05$ keV · b [ref. [39])], 0.63 ± 0.04 keV · b [ref. [41])], 0.56 ± 0.03 keV · b [ref. [42])]. It is still an open question why the activation measurements yield on the average a higher value for $S(0)$ than the direct measurements.

The microscopic potential model also agrees very well with the results of RGM calculations [35,43-45]) which used a more elaborate model space than the one spanned by (2.1), i.e. they considered different oscillator parameters for the two fragments and included excited and rearranged fragmentations. The S-factor as calculated in ref. [43]) is also shown in fig. 5. It shows the best overall agreement with the experimental data for $E \leq 2$ MeV. Kajino and Arima extracted an S-factor in the relevant energy range of $S(10\,\text{keV}) = 0.508$ keV · b. The results of Walliser *et al.* [44,45]) are nearly identical to those of the microscopic potential model except for very low energies ($E \leq 400$ keV) where they predict a slightly higher cross section than the microscopic potential model. Walliser *et al.* obtain an S-factor of $S(0) = 0.598$ keV · b at astrophysically important energies.

It should be emphasized that the microscopically predicted S-factors at astrophysical energies agree well with the value of $S(0) = 0.52 \pm 0.015$ keV · b adopted in the solar model calculations [46]). Since the microscopic studies are able to describe the seven-nucleon system at stellar energies with excellent quality [35,43-45,47,48]) one might put some confidence in the calculated value of $S(0)$ and hence can conclude that the ^{3}He$(\alpha, \gamma)^7$Be reaction is most likely not the source of the solar-neutrino problem.

3.3. The ^{3}H$(\alpha, \gamma)^7$Li REACTION AT STELLAR ENERGIES

The $t(\alpha, \gamma)^7$Li capture process at low energies is very similar to the ^{3}He$(\alpha, \gamma)^7$Be reaction as it is also dominated by E1 capture from the $t+\alpha$ s-wave and d-wave scattering states into two bound states at $E = -2.467$ MeV $(J = \frac{3}{2}^-)$ and $E = -1.99$ MeV $(J = \frac{1}{2}^-)$ in ^{7}Li which can be well approximated as bound states of the $t+\alpha$ system [14,15]). The microscopic potential model calculation of the $t(\alpha, \gamma)^7$Li reaction used this fact by describing the many-body wave functions similar to those of the ^{3}He$(\alpha, \gamma)^7$Be study only converting the isospin quantum numbers in the ^{3}He fragment and by adopting potentials closely related to those used to study the ^{3}He$(\alpha, \gamma)^7$Be reaction. The binding energies of the ^{7}Li bound states and the $P_{3/2}$ and $P_{1/2}$ phase shifts at $E_t \leq 18$ MeV could be well approximated by the following choice of parametrization for the nuclear potential: $W_{I=1} = -95.767$ MeV, $W_s = -1.90$ MeV, $a = 0.7$ fm and $R = 2$ fm for the central part and $R = 1.83$ fm for the spin-orbit part. The s-wave and d-wave scattering states were derived from the Friedrich potential [16]) replacing the depth of the long-ranged gaussian by -38.5 MeV.

The ^{3}H$(\alpha, \gamma)^7$Li E1 capture cross sections at energies $E = 0.1$-1 MeV were calculated from (3.5)-(3.7) using the relative wave functions as derived from (2.2) with potentials mentioned above. The cross sections are shown in fig. 6 in terms of the

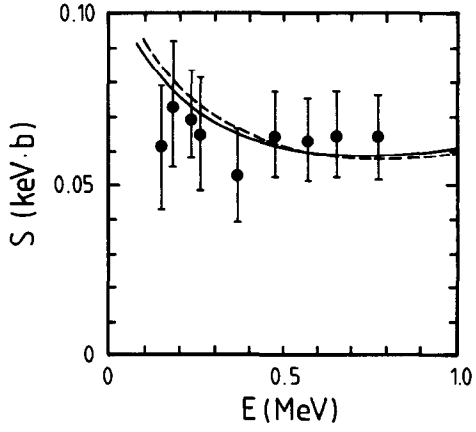

Fig. 6. Comparison of the ^{3}H$(\alpha, \gamma)^7$Li astrophysical S-factors at stellar energies calculated in the present model (solid line) and in the RGM calculation (dashed line, ref. [35])) with the experimental data [49]).

astrophysical S-factor. The agreement with the experimental data of ref. [49]) is good. The microscopic potential model results also agree with those of more elaborate RGM studies thus supporting the conclusions given in refs. [35,43]).

It should be emphasized that the present calculation as well as the RGM studies of refs. [35,43]) yield astrophysical S-factors which differ from the S-factor used to derive the recommended thermally averaged $^3\mathrm{H}(\alpha, \gamma)^7\mathrm{Li}$ reaction rate [33]) in two important points:

(i) The S-factor is increasing for $E \to 0$, while ref. [33]) assumed the S-factor to be energy-independent;

(ii) The S-factor at astrophysically important energies ($E \leq 150$ keV) is noticeably higher than assumed in ref. [33]) which adopted $S(0) = 0.064$ keV · b.

We have derived a thermally averaged $^3\mathrm{H}(\alpha, \gamma)^7\mathrm{Li}$ reaction rate on the basis of an astrophysical S-factor which is the averaged value of the results of ref. [35]) and the present calculation. The S-factor found in ref. [43]) has not been considered in the average since its form of presentation did not allow for its accurate determination from the figures of ref. [43]). However, its overall behaviour agrees well enough with the results of the two other calculations that we do not expect that our thermally averaged reaction rate will be altered drastically if the results of ref. [43]) were included. Defining an effective S-factor at low energies in the standard expansion [33]) and averaging over a Maxwell–Boltzmann distribution for the relative velocity in the entrance channel yields a reaction rate of

$$N_A\langle\sigma v\rangle = 8.672 \times 10^5 T_9^{-2/3} \exp\{-8.080/T_9^{1/3}\} \times \{1 + 0.0525 T_9^{1/3} - 0.448 T_9^{2/3} - 0.165 T_9 + 0.144 T_9^{4/3} + 0.1344 T_9^{5/3}\} \quad [\mathrm{cm^3\,s^{-1}\,mole^{-1}}]. \tag{3.8}$$

Compared with the rate given by Fowler *et al.* [33]) the $^3\mathrm{H}(\alpha, \gamma)^7\mathrm{Li}$ reaction rate as defined in eq. (3.8) is increased at astrophysically important temperatures $T_9 \leq 1$, ranging from $\approx 20\%$ at $T_9 = 1$ to $\approx 60\%$ at $T_9 = 0.1$. Hence the production of $^7\mathrm{Li}$ during the big bang might be appreciably higher than currently believed. This might have an interesting effect on the determination of the nucleon-to-photon ratio and subsequently of the critical density attributed to nucleons within the standard hot big bang model, since these quantities are partly determined by the $^7\mathrm{Li}$ production rate [50,51]).

Finally we have tested the sensitivity of the $^3\mathrm{He}(\alpha, \gamma)^7\mathrm{Be}$ and $^4\mathrm{He}(t, \gamma)^7\mathrm{Li}$ cross sections on the internal structure of the fragments by setting in (3.7) the coefficients $(\mu_N) = 1$ for $N > 3$ and all l. The obtained "non-microscopic" cross sections agree very well with the results obtained in the full microscopic calculation. The reason for this is that the $^3\mathrm{He}(\alpha, \gamma)^7\mathrm{Be}$ and $^4\mathrm{He}(t, \gamma)^7\mathrm{Li}$ reactions at stellar energies are non-resonant. Consequently the relative wave functions $\tilde{g}_{l=0,2}$ are strongly suppressed in the nuclear internal region resulting in very small expansion coefficients $\langle u_N^l \,|\, \tilde{g}_{l=0,2}\rangle$ in (3.7) for those u_N^l with small N corresponding to $(\mu_N) \neq 1$. Note that this is

different for the resonant $^{12}C(p, \gamma)^{13}N$ reaction at stellar energy, since for this process the resonant relative wave functions have significant overlap also with those u_N^l belonging to small N [ref. [52])].

4. Concluding remarks

We have studied the astrophysically important $^2H(\alpha, \gamma)^6Li$, $^3H(\alpha, \gamma)^7Li$ and $^3He(\alpha, \gamma)^7Be$ reactions at stellar energies in the framework of a microscopic potential model. This model is microscopic in the sense that it is based on antisymmetrized many-body wave functions which are chosen in accordance with the results of microscopic many-body reaction theories like resonating group method and generator coordinate method. On the other hand, the model resembles the flexibility of a phenomenological potential model as the nucleus-nucleus potential is adjusted to reproduce experimental data relevant for the studied reaction at stellar energies. Due to this combination of microscopic character and phenomenological flexibility the microscopic potential model can be viewed as a reasonable tool for a physically accurate and consistent description of astrophysically important reactions.

The electromagnetic capture cross sections calculated in the microscopic potential model reproduce the experimental data at low energies for all three reactions considered in the present paper, including the resonant capture from the first excited ^6Li state. The present results also agree with elaborate calculations of the $^3H(\alpha, \gamma)^7Li$ and $^3He(\alpha, \gamma)^7Be$ cross sections in the framework of the RGM. To our knowledge there is no RGM study of the resonant $^2H(\alpha, \gamma)^6Li$ reaction.

Possible astrophysical consequences of the present calculation can be summarized as follows:

(i) Our study supports the commonly accepted idea that only a very small amount of ^6Li has been produced in the big bang.

(ii) Due to the good agreement between experiment and theory it is unlikely that the $^3He(\alpha, \gamma)^7Be$ reaction is the source of the solar neutrino problem.

(iii) In agreement with two RGM calculations we predict an energy-dependent astrophysical S-factor for the $^3H(\alpha, \gamma)^7Li$ reaction which is higher at stellar energies than currently accepted. On the basis of the microscopic studies we recommend a thermally averaged reaction rate which predicts a noticeably higher production of ^7Li during the big bang.

References

1) K. Wildermuth and Y.C. Tang, A unified theory of the nucleus (Vieweg, Braunschweig, 1977)
2) Y.C. Tang, M. LeMere and D.R. Thompson, Phys. Reports **47** (1978) 167
3) K. Langanke and H. Friedrich, Microscopic description of nucleus-nucleus collisions, in Advances in Nuclear Physics, vol. 17, ed. J. Negele and E. Vogt (Plenum, New York, 1986)
4) K. Langanke and S.E. Koonin, Nucl. Phys. **A410** (1983) 334
5) K. Langanke and S.E. Koonin, Nucl. Phys. **A439** (1985) 384; **A448** (1986) 764
6) W.A. Fowler, Rev. Mod. Phys. **56** (1984) 149

7) F.K. Thielemann, Adv. Space Res. **4** (1984) 67
8) S.E. Woosley, Proc. Accelerated radioactive beams Workshop, ed. L. Buchmann and J.M. D'Auria (Triumf, Vancouver, 1985)
9) P. Dyer and C.A. Barnes, Nucl. Phys. **A233** (1974) 495
10) K.U. Kettner, H.W. Becker, L. Buchmann, J. Görres, H. Kräwinkel, C. Rolfs, P. Schmalbrock, H.P. Trautvetter and A. Vlieks, Z. Phys. **A308** (1982) 73
11) A. Redder, H.W. Becker, J. Görres, M. Hilgemeier, A. Krauss, C. Rolfs, U. Schröder, H.P. Trautvetter, K. Wolke, T.R. Donoghue, T.C. Rinckel and J.W. Hammer, Phys. Rev. Lett. **55** (1985) 1262
12) C. Funck, K. Langanke and A. Weiguny, Phys. Lett. **152B** (1985) 11
13) H. Kanada, T. Kaneko, S. Saito and Y.C. Tang, Nucl. Phys. **A444** (1985) 209
14) H. Kanada, Q.K.K. Liu and Y.C. Tang, Phys. Rev. **C22** (1980) 813
15) R.D. Furber, R.E. Brown, G.L. Peterson, D.R. Thompson and Y.C. Tang, Phys. Rev. **C25** (1982) 23
16) H. Friedrich, Nucl. Phys. **A294** (1978) 81
17) D.A. Zaikine, Nucl. Phys. **A170** (1971) 584
18) S. Saito, Progr. Theor. Phys. Suppl. **62** (1978) 11
19) H. Friedrich, Phys. Reports **74** (1981) 209
20) H. Friedrich and K. Langanke, Phys. Rev. **C28** (1983) 1385
21) D. Baye and P. Descouvemont, Ann. of Phys., in print
22) D. Wintgen, H. Friedrich and K. Langanke, Nucl. Phys. **A408** (1983) 239
23) H.P. Brall, diploma thesis (Münster, 1982)
24) L.C. McIntyre and W. Haeberli, Nucl. Phys. **A91** (1967) 382
25) D. Baye and P. Descouvemont, Nucl. Phys. **A407** (1983) 77
26) Y. Suzuki, Progr. Theor. Phys. **55** (1976) 1751
27) H.J. Assenbaum, K. Langanke and A. Weiguny, Z. Phys. **A318** (1984) 35
28) D.N. Schramm and R.V. Wagoner, Ann. Rev. Nucl. Sci. **27** (1977) 37
29) W.A. Fowler, as quoted in ref. [30])
30) R.G.H. Robertson, P. Dyer, R.A. Warner, R.C. Melin, T.J. Bowles, A.B. McDonald, C.C. Ball, W.G. Davies and F.D. Earle, Phys. Rev. Lett. **47** (1981) 1867
31) B. Jenny, W. Grübler, V. König, P.A. Schmelzbach and C. Schweizer, Nucl. Phys. **A397** (1983) 61
32) F. Ajzenberg-Selove, Nucl. Phys. **A413** (1984) 1
33) W.A. Fowler, G.R. Caughlan and B.A. Zimmerman, Ann. Rev. Astron. Astrophys. **13** (1975) 69
34) J. N. Bahcall and R. Davis Jr., in Essays in nuclear astrophysics, ed. C.A. Barnes, D.D. Clayton and D.N. Schramm (Cambridge University Press, New York, 1982) p. 243
35) T. Mertelmeier and H.M. Hofmann, to be published
36) R.J. Spiger and T.A. Tombrello, Phys. Rev. **163** (1967) 964
37) P.D. Parker and R.W. Kavanagh, Phys. Rev. **131** (1963) 2578
38) K. Nagatani, M.R. Dwarakanath and D. Ashery, Nucl. Phys. **A128** (1969) 325
39) J.L. Osborne, C.A. Barnes, R.W. Kavanagh, R.M. Kremer, G. J. Mathews, J.L. Zyskind, P.D. Parker and A.J. Howard, Phys. Rev. Lett. **48** (1982) 1664; Nucl. Phys. **A419** (1984) 115
40) T.K. Alexander, G.C. Ball, W.N. Lennard, H. Geissel and H.B. Mak, Nucl. Phys. **A427** (1984) 526
41) R.G.H. Robertson, P. Dyer, T.J. Bowler, R.E. Brown, N. Jarmie, C.H. Maggiore and S.M. Austin, Phys. Rev. **C27** (1983) 11
42) H. Volk, H. Kräwinkel, R. Santo and L. Wallek, Z. Phys. **A310** (1983) 91
43) T. Kajino and A. Arima, Phys. Rev. Lett. **52** (1984) 739
44) H. Walliser, Q.K.K. Liu, H. Kanada and Y.C. Tang, Phys. Rev. **C28** (1983) 57
45) H. Walliser, H. Kanada and Y.C. Tang, Nucl. Phys. **A419** (1984) 133
46) J.N. Bahcall, W.F. Hübner, S. H. Lubow, P.D. Parker and R.K. Ulrich, Rev. Mod. Phys. **54** (1982) 767
47) T. Kajino, T. Matsuse and A. Arima, Nucl. Phys. **A413** (1984) 323
48) T. Kajino, T. Matsuse and A. Arima, Nucl. Phys. **A414** (1984) 185
49) G.M. Griffiths, R.A. Morrow, P.J. Riley and J.B. Warren, Can. J. Phys. **39** (1961) 1387
50) A.M. Boesgaard and G. Steigman, Ann. Rev. Astron. Astrophys. **23** (1985) 319
51) J. Yang, M.S. Turner, G. Steigman, D.N. Schramm and K.A. Olive, Astr. J. **281** (1984) 493
52) K. Langanke, O.S. van Roosmalen and W.A. Fowler, Nucl. Phys. **A435** (1985) 657; **A446** (1985) 750